Mechanism of Primary Frequency Regulation for Battery Hybridization in Hydropower Plant

Yiwen Liao, *Student Member*, *IEEE*, Weijia Yang, *Member*, *IEEE*, Zhecheng Wang, *Student Member*, *IEEE*, Yifan Huang, *Student Member*, *IEEE*, and C. Y. Chung, *Fellow*, *IEEE*

***Abstract*—Battery hybridization in hydropower plants is a hydropower flexibility enhancement technology innovation that can potentially expand hydropower's contributions to the grid, but its fundamental characteristics and influencing mechanisms are still unclear. In this paper, primary frequency regulation (PFR) performance and the mechanism of this new technology are studied. A battery hybridized hydropower plant (BH-HPP) model, based on a field-measured-data-based hydropower plant (HPP) model and a verified battery simplified model, is established. Analysis of system stability and dynamics is undertaken for three different battery control strategies by root locus and participation factor methods. Compared to conventional HPPs, analysis results theoretically reveal BH-HPP can not only accelerate system regulation rapidity but also effectively enlarge HPP stability region during PFR process. Time domain simulation verifies the results and further shows synthetic control has better performance among introduced strategies. Besides, initial design ranges of control parameters considering battery capacity and a renewable energy source scenario case are also discussed. This work could provide theoretical support for flexibility enhancement solutions for hydropower systems.**

***Index Terms*—Battery hybridization, dynamic response, hydropower plant, primary frequency regulation, stability.**

I. Introduction

At present, power system structures are undergoing notable changes due to the rapid development of intermittent renewable energy sources (RESs), e.g., wind and solar energy [1]. As one of the main regulating power sources of the grid, hydropower is going to be called upon more to compensate for RES integration, which means more frequent regulation action of hydropower plants (HPPs), as well as a heavier burden on hydropower units [2], [3].

Therefore, the most pressing concern for HPPs is how to enhance regulating capability while reducing wear and tear on units. In addition to seeking optimization of existing HPPs, some flexibility enhancement technology innovations are also being explored. One of these is the cooperative regulation of HPPs (or hydropower units) with batteries. This new technology has been investigated within the frame of the European project XFLEX Hydro [4]. In a hydropower retrofit program called HydroWIRES initiated by the U.S. Department of Energy, some fast response energy storage devices including batteries are also planned to be installed on the power source side to help enhance the flexibility of run-of-river (ROR) HPPs [5]. German utility RWE also recently embarked on a project that includes the integration of massive battery energy storage systems (ESSs) with ROR-HPPs [6]. Being in the infancy, further research on the use of batteries to improve grid ancillary service capability of HPPs on the power source side is needed, especially these flexibility enhancement technologies for hydropower that have not yet taken off in most countries.

In the future, the 'regulator' role of HPPs may even exceed their role as 'power sources'. Frequency regulation is an important function of HPPs as grid regulators, and their performance not only affects a power plant's revenue, but also directly affects power system security [3]. The frequency regulation performance of HPPs is mainly reflected in two aspects: stability and rapidity. Ensuring stability is an especially important prerequisite. The negative damping effects induced by fast regulation of governors and water hammers are the key reason for instability and ultra-low frequency oscillations (ULFOs) of the grid (frequently occurring in hydropower-dominant systems) [7]–[9]. However, governors are usually set to be extremely sensitive in many HPPs to pursue better primary frequency regulation (PFR) response performance, and it further aggravates the risk of ULFOs. Consequently, efforts to ensure the stability and rapidity of hydropower systems are often in contradiction. To address the problem, considerable research has been carried out. For example, the influence of different control modes on the regulation quality of HPPs is analyzed in [10], while the governor parameters are adjusted in [11]. Besides, multi-objective optimization methods and some novel strategies have been used to mitigate the contradictory relationship between the negative damping effect of hydropower units and the rapid response of PFR [12]–[14]. Although the above works enhance frequency regulation performance, they are only improvements in terms of control strategies. Nonetheless, inherent characteristics of the hydropower system structure make it difficult to fundamentally solve the contradiction between stability and rapidity. For HPPs at high-voltage direct current (HVDC) sending termi-

Manuscript received May 3, 2022; revised September 22, 2022; accepted November 24, 2022. Date of online publication April 20, 2023; date of current version May 29, 2023. This work was supported in part by the National Natural Science Foundation of China under No. 52079096.

Y. W. Liao, W. J. Yang (corresponding author, email: weijia.yang@whu.edu.cn; ORCID: https://orcid.org/0000-0003-1638-0792), Z. C. Wang and Y. F. Huang are with the State Key Laboratory of Water Resources and Hydropower Engineering Science, Wuhan University, Wuhan 430072, China.

C. Y. Chung is with the Department of Electrical Engineering, The Hong Kong Polytechnic University, Hong Kong, China.

DOI: 10.17775/CSEEJPES.2022.06420

2096-0042 © 2022 CSEE. This is an open access article under the CC BY-NC-ND license (http://creativecommons.org/licenses/by-nc-nd/4.0/).

nals, a frequency limitation controller (FLC) seems to be a feasible method [15], [16]. However, it is difficult to extend this approach to more common AC power systems because of the 'DC system only' feature.

This further underscores the importance of developing flexibility enhancement technology innovations for hydropower systems to improve the provision of grid services. Integrating with fast response ESSs is a viable new conceptual design of hydropower facilities by retrofitting existing conventional units (even large capacity units) [17], which means it has potential to be promoted in HPPs. Studies on hydropower units integrated with flywheels [18], [19] and supercapacitors [20], [21] to improve frequency regulation capability have been carried out in the past few years, but minimal research has been conducted on the synergistic frequency regulation of batteries and hydropower units. The benefits of the combined operation of hydropower units and batteries in power regulation mode are investigated in [22], but the dynamic characteristic of the more common frequency control mode in PFR is ignored. A wear and tear evaluation research in Kaplan turbines coupled with batteries is introduced in [4] and has been conducted on a prototype. A model predictive control strategy for HPP hybridized with a large enough battery is proposed in [23] to reduce penstock fatigue, but battery capacity has been neglected. Two complementary methods for a combination of pumped storage plant with battery are discussed in [24], while the hydraulic transient process is simplified into ramp rates. In short, existing research focuses more on applied control strategy, but how this new technology affects the original hydropower system has not been revealed. Moreover, most current works have been conducted for synergistic operation on the grid side and system level [25]–[27] instead of on the power source side, or unit side.

To sum up, studies on the mechanism of cooperative regulation of battery hybridization in hydropower plants (a unit side enhancement) are needed, as it is exactly what the technology lacks at present, and a theoretical basis for subsequently improving source-grid coordination of the power system in the future. Hence, the main contributions of this paper are to reveal the mechanism of battery-hybridized hydropower plants (BH-HPPs) and explore characteristics of common-used battery control strategies; the PFR dynamic process and performance of a BH-HPP are studied, especially focusing on how the battery affects the stability and rapidity of the hydropower system.

The paper is composed of six sections including the introduction. The model of the BH-HPP is established in Section II. Stability analysis is performed in Section III. Section IV explores the main influences on the system. Time domain response analysis is performed in Section V. Section VI discusses the performance improvements of the BH HPP in the PFR process, and Section VII concludes.

II. Mathematical Model

This paper focuses on a BH-HPP for frequency regulation. As shown in Fig. 1, the power source side hydropower flexibility enhancement is achieved by hybridizing a small-size battery in parallel to the hydropower unit's busbar before power is integrated and delivered to the grid through the generator step-up transformer. In this section, a small-signal mathematical model of the system for PFR is established.

A. PFR Model for Hydropower System

The hydropower system generally consists of an actuator, penstock, Francis hydraulic turbine, generator, loads, and a proportional-integral (PI) governor [28], [29]. As the unit is in the frequency control mode during PFR, guide vane opening (GVO) is the feedback for the governor. Hence, the governor equation is:

$$(1+b_pK_p)\frac{\mathrm{d}\Delta y_{PI}}{\mathrm{d}t}+b_pK_i\Delta y_{PI}=-K_p\frac{\mathrm{d}\Delta\omega}{\mathrm{d}t}-K_i\Delta\omega \tag{1}$$

where b_p is the droop coefficient of the governor; K_p and K_i are respectively, the proportional gain and integral gain of the governor; y_{PI} is the PI governor output signal; and ω is system frequency.

The actuator model, penstock model based on the second-order elastic water hammer equation, and the linear Francis hydraulic turbine model based on transfer coefficients can be expressed as (2) to (4), respectively:

$$T_y\frac{\mathrm{d}\Delta y}{\mathrm{d}t}=\Delta y_{PI}-\Delta y \tag{2}$$

$$\frac{\Delta h}{\Delta q}=\frac{-T_ws}{1+\alpha T_e^2s^2} \tag{3}$$

$$\begin{cases}\Delta P_m=e_y\Delta y+e_\omega\Delta\omega+e_h\Delta h\\ \Delta q=e_{qy}\Delta y+e_{q\omega}\Delta\omega+e_{qh}\Delta h\end{cases} \tag{4}$$

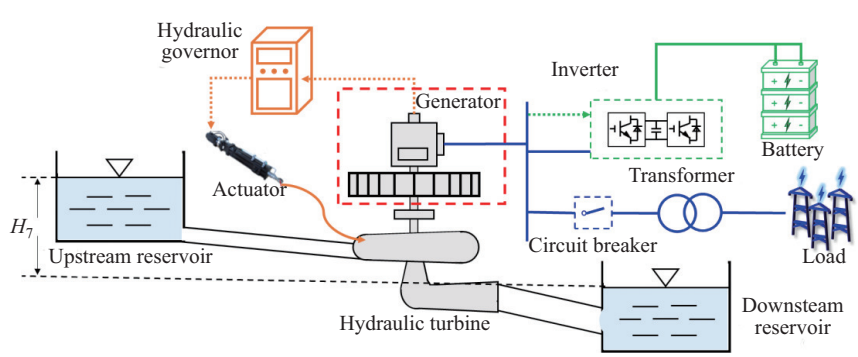

Fig. 1. Battery-hybridized hydropower plant (BH-HPP).

where e_y, e_h, e_ω are partial derivatives of turbine power output with respect to guide vane opening, head, and speed; e_{qy}, e_{qh}, $e_{q\omega}$ are partial derivatives of turbine discharge with respect to guide vane opening, head, and speed; h is water head; q is flow; s is Laplace operator; T_e is time constant of water column elasticity; T_y is servo time constant; T_ω is water starting time constant; and α is elastic coefficient of the penstock; y is actuator stroke.

A single machine with loads in an isolated grid, which is a hazardous operating condition detrimental to stability, is set as a research scenario in this paper. Generator and loads can then be approximated by the first-order rotor equation of motion as:

$$T_a \frac{\mathrm{d}\Delta\omega}{\mathrm{d}t} = \Delta P_m - \Delta P_e - e_g \Delta\omega \tag{5}$$

where e_g is the change rate of the generator load torque with speed; P_m and P_g are respectively, output torque of hydropower unit and electromagnetic torque of loads; and T_a is rotor inertia time constant.

The basic dynamic process of HPPs can be fully described by (1) to (5). Taking $\Delta x = [\Delta h, \Delta\dot{h}, \Delta\dot{y}_{PI}, \Delta y, \Delta\omega]^{\mathrm{T}}$ as state variables, the state space model of the isolated hydropower system can be written as (6), where A_1 is a 5×5 state matrix:

$$\Delta\dot{x} = A_1 \Delta x \tag{6}$$

Consequently, the block diagram of the isolated hydropower system model shown in Fig. 2 is obtained, where $G_i(s)$ is the transfer function corresponding to each subsystem (without expanded derivation in the text).

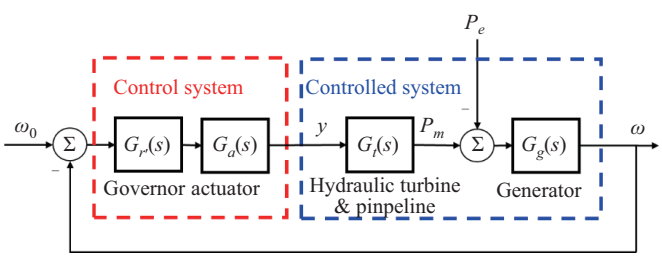

Fig. 2. Block diagram of the isolated hydropower system.

The open-loop transfer function and the overall transfer function in frequency control mode are then as follows:

$$G_{oh}(s) = -G_g(s)G_{r'}(s)G_a(s)G_t(s) \tag{7}$$

$$G(s) = \frac{\omega(s)}{P_e(s)} = -\frac{b_0 s^4 + b_1 s^3 + b_2 s^2 + b_3 s + b_4}{a_0 s^5 + a_1 s^4 + a_2 s^3 + a_3 s^2 + a_4 s + a_5} \tag{8}$$

where a_i and b_i are coefficients of the characteristic equation.

B. Frequency Regulating Model for Ancillary Battery

A reduced-order model for the ancillary battery system is applied in this paper to facilitate theoretical analysis, based on the following considerations:

- In the concerned electromechanical transient time scale, some time-varying characteristics of batteries (open-circuit voltage, temperature effects, ramp rate, etc.) can be ignored.
- Compared to the secondary frequency regulation (SFR) reserve of the battery, its PFR reserve is small, implying little change of state of charge (SOC) during PFR merely has a slight impact on the battery performance.
- Except for power response, the type, SOC management, degradation, as well as the advanced controller of the battery, are not the concerned issue of this work.
- Power capacity of the ancillary battery is expected to be about 5% (even lower) of that of the unit, but it does not affect models and analysis. More discussion on battery capacity can be seen in Section V.

The battery converter is controlled by a classical dual closed-loop strategy, the power outer-loop of which responds to frequency variation $\Delta\omega$ and generates current inner-loop input (active power command ΔP_{bset}). The outer-loop control includes a proportional term and a derivative term, which can represent the most commonly used control methods in the industry. The proportional term and gain K_e can be, respectively, regarded as the virtual droop control and unit droop power; similarly, the derivative term and gain M_e can be abstracted as virtual inertia control and unit regulation power. Thus, the outer-loop controller equation is obtained:

$$\Delta P_{\mathrm{bset}} = -M_e \frac{d\Delta\omega}{\mathrm{d}t} - K_e \Delta\omega \tag{9}$$

Here, the inner loop is simplified to a first-order transfer function [30], in which the external response characteristics of the controller and battery are reflected by a storage response time constant T_{pb} (typically 0.1 s), as shown in (10):

$$T_{pb} \frac{\mathrm{d}\Delta P_b}{\mathrm{d}t} + \Delta P_b = \Delta P_{\mathrm{bset}} \tag{10}$$

where P_b is charge or discharge power of the battery.

Because the frequency regulation strategy can be altered to a single (virtual droop or virtual inertia) or a synthetic control strategy, the outer-loop controller equation should be adapted to the specific condition.

C. Model Verification

In this section, verifications of the HPP and battery models are presented. Measured data of a large HPP in China, which is planning to be equipped with batteries to help its units avoid vibration zones, is used to validate the hydropower model. Although HPP in the real world is a complex nonlinear system, its dynamics in small-disturbance conditions can be simplified to a linear process [31]. As shown in Fig. 3, this conclusion

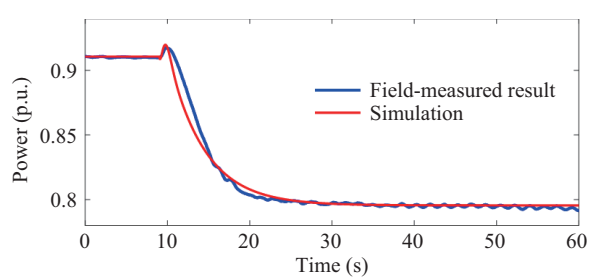

Fig. 3. Comparison between simulation and a field-measured result of the HPP.

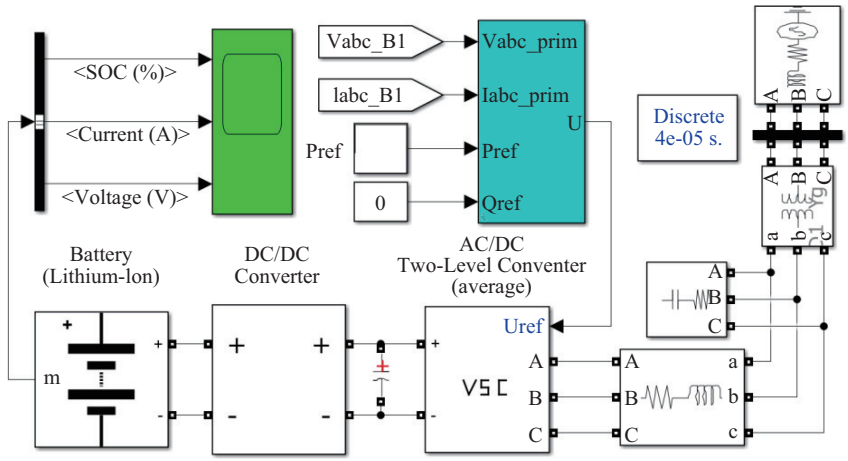

Fig. 4. Schematic diagram of the SPS model of the battery.

was verified again by good consistency between the introduced model's numerical simulation and a field-measured result of the plant in a grid-connected frequency disturbance condition, which illustrates sufficient accuracy of the hydropower model.

Verification of the battery is conducted by comparing active power response from the introduced first-order model and a SimPowerSystems (SPS) model. The SPS model is based on a standard generic battery block in MATLAB/SPS, and the Lithium-Ion type is adopted in the verification. The model includes a detailed representation of power electronic converters by modeling a DC/DC converter, a two-level DC/AC converter, and a complete dual closed-loop control strategy. Fig. 4 is the schematic diagram.

Comparison is shown in Fig. 5. Generally, simulations of rapid power response by the first-order model have good agreement with the result from the SPS model, which shows the reliability of the simplified battery model. The main difference occurs in fluctuation and noise, which is expected, as merely the battery's rapidity was considered in the simplified model, while it does not matter in the focused time scale.

D. Integrated System

The integrated system model with input ΔP_e and output $\Delta\omega$ can be obtained, as shown in Fig. 6. Hence, the open-loop transfer function and overall transfer function are given as (11) and (12).

$$G_o(s) = -G_g(s)\cdot[G_c(s)\cdot G_b(s) + G_t(s)\cdot G_r(s)] \tag{11}$$

$$G(s) = -\frac{b_0 s^5 + b_1 s^4 + b_2 s^3 + b_3 s^2 + b_4 s + b_5}{a_0 s^6 + a_1 s^5 + a_2 s^4 + a_3 s^3 + a_4 s^2 + a_5 s + a_6} \tag{12}$$

Taking $\Delta x = [\Delta h, \Delta\dot{h}, \Delta\dot{y}_{PI}, \Delta y, \Delta\omega, \Delta P_b]^{\mathrm{T}}$ as state variables, the state space model of the integrated system can be written as (13), where A_2 is a 6×6 state matrix:

$$\Delta\dot{x} = A_2\Delta x \tag{13}$$

Note the equations should be adapted to the frequency regulation strategy. For example, the numerator order of (12) changes to fourth under virtual droop control, and the state matrix of (13) changes accordingly. Table I shows general system parameter values, on which the whole work is based.

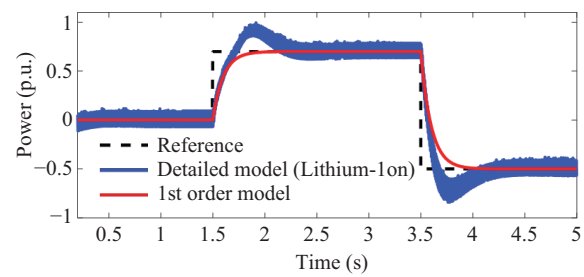

Fig. 5. Comparison between first-order model and detailed SPS model of the battery.

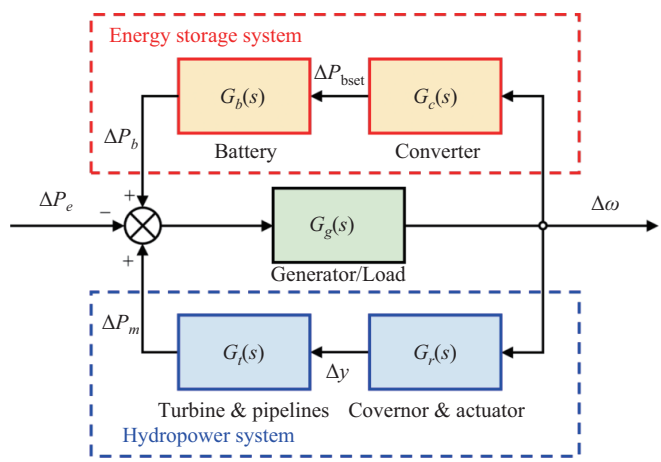

Fig. 6. Integrated system model.

TABLE I
SYSTEM PARAMETER VALUES

Parameter	Value	Parameter	Value	Parameter	Value
T_w	1.28 s	T_y	0.2 s	K_e	2.5
T_e	0.49 s	T_a	10.25 s	M_e	5.0
α	0.5 s	e_g	0	e_y, e_h, e_ω	0.5, 1.5, −1.0
b_p	0.02 s	T_{pb}	0.1 s	$e_{qy}, e_{qh}, e_{q\omega}$	0.8, 0.5, 0

III. STABILITY ANALYSIS

In this section, the isolated HPP system is set to a critically stable condition ($K_p = 8.0$, $K_i = 1.5$) as the standard condition to examine the effects of different battery control

strategies on the stability of HPPs. As mentioned in Section II, the battery control strategy is based on proportional and differential terms, as well as their combinations. Integral outer-loop control with the function to mainly eliminate steady-state error is not considered, because HPP is a system with steady-state error. If an integral term is applied, the battery will partially replace the SFR task to remain charging or discharging, which is a substantial challenge to an ancillary small-sized battery.

A. Proportional Control

When only the proportional control strategy is applied, outer-loop controller equation changes to $\Delta P_{\text{bset}} = -K_e \Delta\omega$, and proportional gain K_e is set to 2.5. The Bode diagrams of the isolated HPP system and the BH-HPP are drawn from (7) and (11), as shown in Fig. 7(a). The Bode diagrams show battery ancillary regulation with proportional control notably reduces amplitude response in low-frequency band compared to the isolated HPP system, which implies the steady-state error is reduced, and it is because the HPP in frequency regulation mode is a constant-target system. For medium-frequency band, battery regulation with proportional control slows down the rate of amplitude-frequency characteristic and shifts cut-off frequency to the left, while the phase-frequency characteristic has a notable increase. This greatly increases phase margin, improves system stability, and reduces overshoot, as well as regulation time, indicating the system has better dynamic performance to low-frequency oscillation signals. In other words, it reflects the virtual droop (damping) characteristics of the battery with proportional control.

To visualize the effects of a battery on the stability of HPP, stable regions of governor parameters ($K_p - K_i$) for HPP and BH-HPP are obtained from (8) and (12) based on the Hurwitz stability criterion [32], [33]. Fig. 7(b) shows PFR with battery virtual droop control vastly widens the stable region (red), creating a large stability margin, especially in K_i direction, so the initial HPP operating condition ("◯"), which is critically stable, is re-integrated into a more stable region. Abbreviation 'OP' refers to the operating point of the hydropower unit.

B. Derivative Control

When only the derivative control strategy is applied, the outer-loop controller equation is $\Delta P_{\text{bset}} = -M_e \Delta\dot{\omega}$, and derivative gain M_e is set to 5.0. Fig. 8(a) presents the Bode diagrams of HPP and BH-HPP in battery derivative control. Unlike with virtual droop control, the Bode diagram shows

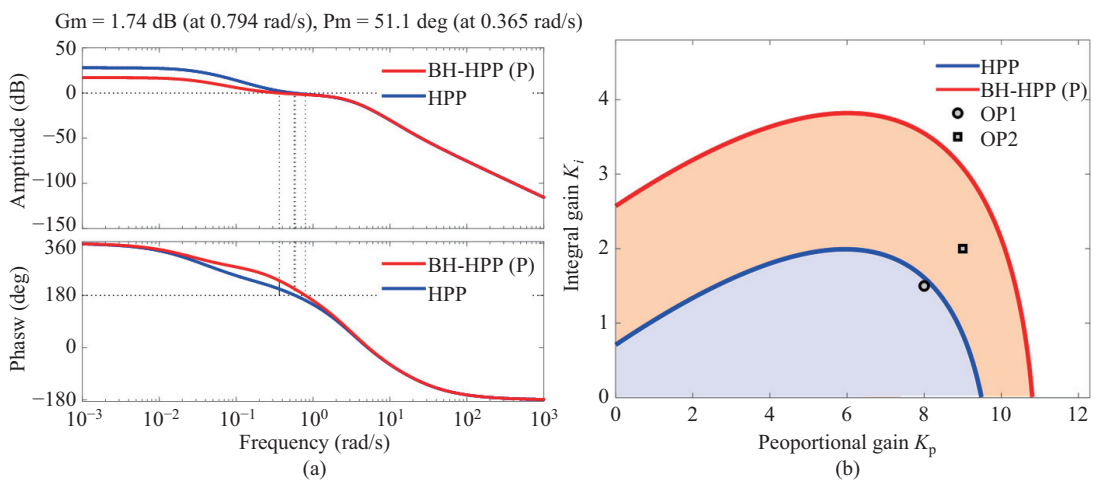

Fig. 7. Bode diagrams (a) and stable regions (b) of HPP and BH-HPP in proportional control.

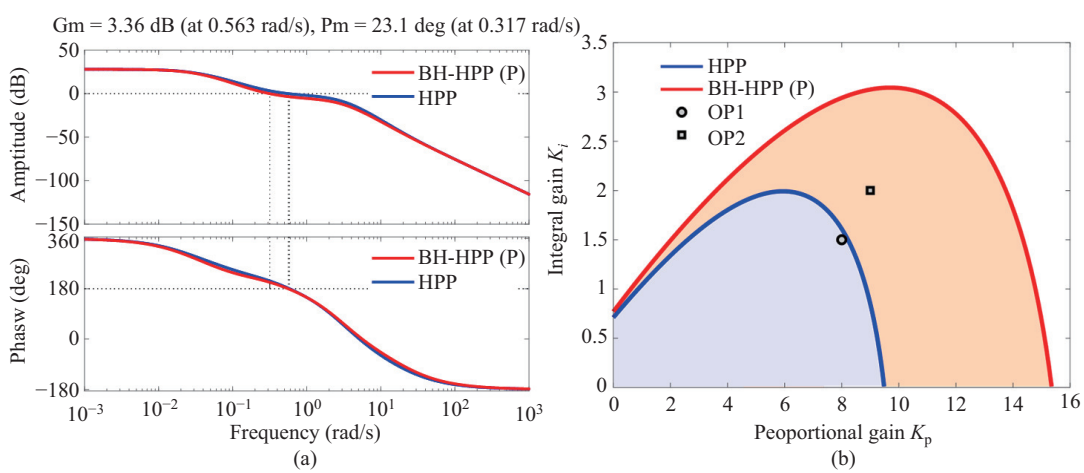

Fig. 8. Bode diagrams (a) and stable regions (b) of HPP and BH-HPP in derivative control.

battery ancillary regulation with derivative control mainly affects the medium-frequency band: amplitude-frequency characteristic slightly shifts to the left, while phase-frequency characteristic decreases slightly. This reflects an inertia effect. Although the overall dynamic performance of the system is slightly reduced, stability to maintain constant values is improved. The slight decrease in amplitude-frequency characteristics also indicates the system's immunity to interference is enhanced, and the affected band depends on the rapidity of the battery.

Similarly, stable regions of HPP and BH-HPP in derivative control are obtained based on the Hurwitz stability criterion. Fig. 8(b) shows frequency regulation with battery virtual inertia control also notably widens thestable region, especially in K_p direction (red), which means a larger adjustable space for governor proportional gain. Moreover, the critically stable HPP operating condition ("◯") is re-integrated into the more stable region, as well.

C. Synthetic Control

When synthetic control strategy is applied, the outer-loop controller equation is as (9), where $K_e = 2.5$, $M_e = 5.0$. Fig. 9(a) shows the Bode diagrams in synthetic control. Frequency characteristics of BH-HPP with synthetic control are the superposition of those for virtual droop control and virtual inertia control. The system not only can respond quickly in the initial stage after frequency changes but also improve steady-state performance, as well as interference immunity. The stable region shown in Fig. 9(b) is greatly extended in both K_p and K_i directions.

IV. Influence Mechanism Analysis

A. Analysis of Battery Control Parameters

To further examine the effects of battery control on PFR performance, parameter root loci of BH-HPPs for the three strategies are investigated, as shown in Fig. 10.

Figure 10(a) shows the root loci of dominant poles when K_e increases from zero in virtual droop control. The original HPP is in ULFO. As K_e increases, conjugate dominant poles move away from the imaginary axis and the ULFO area, showing a beneficial trend to system stability; the negative real pole gradually tends to the imaginary axis, but it eventually stagnates at a position left of the imaginary axis.

Figure 10(b) shows the root loci of dominant poles when M_e increases from zero in virtual inertia control. As M_e increases, conjugate dominant poles first move away from the imaginary axis rapidly, then converges at a slower speed after

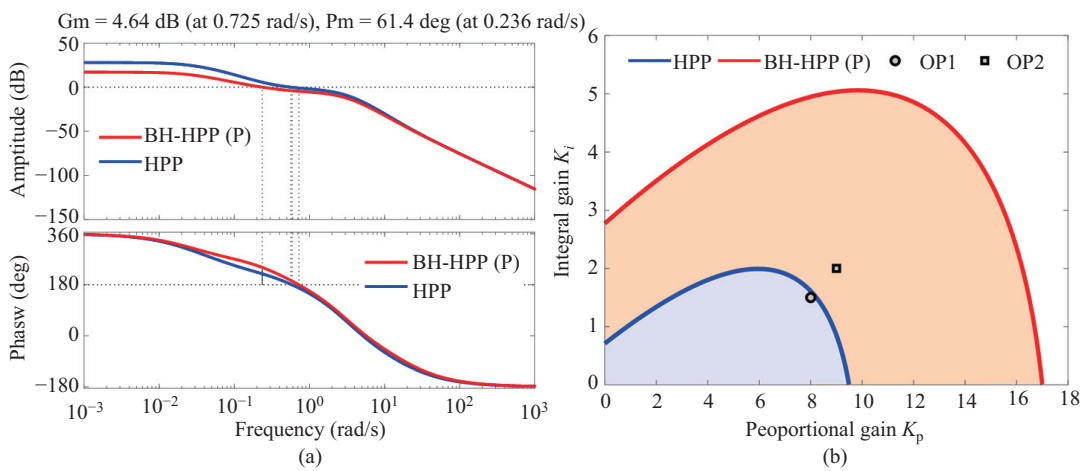

Fig. 9. Bode diagrams (a) and stable regions (b) of HPP and BH-HPP in synthetic control.

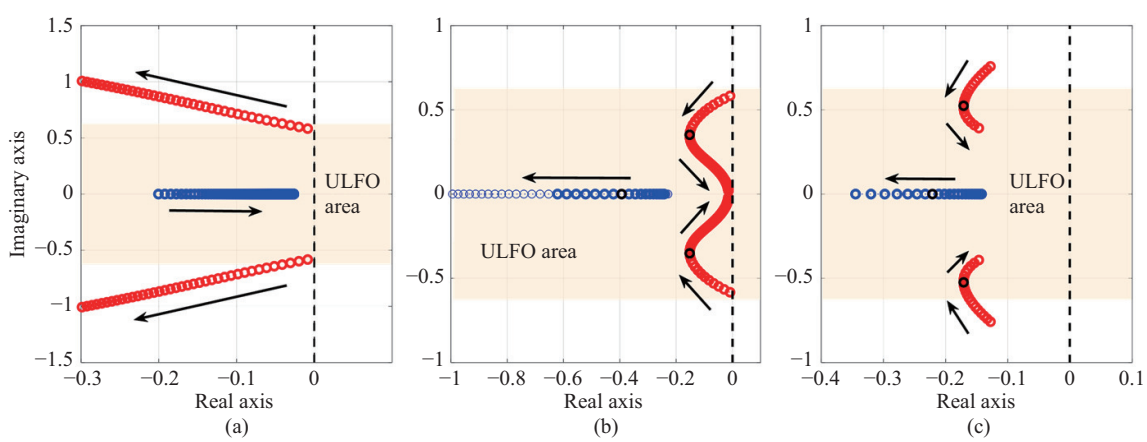

Fig. 10. Root locus of (a) K_e, (b) M_e, and (c) a_m.

an inflection point; the negative real pole shows a trend of moving away from the imaginary axis, first slowly and then quickly. Gradually, only conjugate poles remain as dominant poles (the light blue one is no longer dominant pole), and the system moves deeply into the ULFO area, implying that huge inertia (including water flow inertia, unit inertia, and virtual inertia) is likely to be the cause of ULFO in hydropower systems. In addition, the root locus shows the damping ratio of a system with too large a value of M_e will become very small, which means an extremely weak anti-interference capacity and a negative impact on stability.

A new parameter, virtual inertia control task coefficient a_m, which needs to satisfy $K_e = (1-a_m)K_{e0}$ and $M_e = a_m M_{e0}$, is proposed to represent the percentage of virtual inertia effect in the integrated strategy. Standard case is set as $K_{e0} = 2.5$, $M_{e0} = 5.0$. Fig. 10(c) shows the dominant poles' root loci of BH-HPP in the synthetic control strategy when a_m changes (0 to 1). As battery virtual inertia effect increases, the change of dominant poles shows a similar trend to Fig. 10(b). However, the addition of virtual droop control means poles have an overall shift to the left, enhancing system stability and also partly reducing risks of ULFO.

B. Analysis of Hydro-battery Coupling Interaction

According to the participation factor method, Equations (14) and (15) need to be satisfied for every eigenvalue. Participation factor p_{ki} is expressed as (16), which reflects the participation degree of kth state variable in i^{th} mode [34].

$$A\varphi_i = \lambda_i \varphi_i \tag{14}$$

$$\psi_i A = \lambda_i \psi_i \tag{15}$$

$$p_{ki} = \varphi_{ki}\psi_{ik} \tag{16}$$

Table II compares participation factors of each state variable of the HPP and three BH-HPPs. The isolated HPP system, which is the standard scenario of this paper, has two oscillation modes: one is the ULFO mode, the dominant mode of the system, which is the so-called governor-dominant mode because governor participation factors of y_{pi} and y are largest; the other is water-elastic-dominant mode because change rate of water head h_1 is the most important.

Compared to HPP, the biggest difference in the BH-HPP is the addition of a negative real pole with a large absolute value; this means greatly improved response dynamic characteristics and a notably shortened settling time. Further, the position of the poles almost depends on battery power output. It fully demonstrates the rapidity advantage of battery ancillary frequency regulation. Another notable difference is the battery greatly reduces the involvement of frequency ω in water-elastic-dominant mode. A comparison of the three BH-HPPs shows, for the governor-dominant mode, actuator stroke y is still the most involved state variable in the virtual droop control system, while governor command y_{pi} is the most important in both virtual inertia control system and synthetic control system. In addition, in the virtual inertia control system, y_{pi} becomes the most critical factor of the negative real dominant pole, and participation of y is also significantly enhanced. This indicates that, for systems with large inertia, such as hydropower systems, governor parameter adjustment is still a highly critical part of the frequency regulation process.

V. Time Domain Response Analysis

Based on the above theoretical analysis results, time domain response analysis of the BH-HPP for PFR is executed in this section by using MATLAB/Simulink software.

A. Frequency Response Characteristics

PFR results of different system responses to step load disturbance are presented in Fig. 11, and simulation OPs are shown in stability regions in Section III. For OP1, the battery not only helps HPP significantly reduce frequency deviation but also quickly stabilizes frequency. Values of PFR performance evaluation indexes are given in Table III, where maximum frequency deviation $\Delta f_{\max}$ reflects damping characteristics (stability), settling time T_s and maximum inverse power output of hydropower unit $\Delta P_{\text{inv}-\max}$ reflect dynamic performance (rapidity), and frequency steady-state error Δf_s reflects steady-state performance of the system (accuracy).

TABLE II
Participation Factors of the HPP and BH-HPPs

System	Parameters	Eigenvalues	ξ	f (Hz)	T (s)	Participation factors						OM
						w	y_{pi}	y	h	h_1	P_b	
HPP	$K_p = 8.0$, $K_l = 1.5$	−0.009+0.583i	0.015	0.093	10.783	0.133	0.911	1.000	0.346	0.038	—	Governor
		−5.093+3.001i	0.862	0.478	2.094	0.700	0.442	0.698	0.509	1.000	—	Water elasticity
		−0.229	1.000	0.000	4.367	1.000	0.301	0.133	0.020	0.000	—	—
HPP & Battery (P)	$K_e = 2.5$	−0.117+0.766i	0.152	0.121	8.292	0.178	0.886	1.000	0.470	0.069	0.022	Governor
		−5.133+3.088i	0.861	0.483	2.071	0.030	0.451	0.690	0.516	1.000	0.036	Water elasticity
		−0.141	1.000	0.000	7.092	1.000	0.514	0.148	0.013	0.000	0.007	—
		−9.791	1.000	0.000	0.102	0.022	0.004	0.004	0.003	0.006	1.000	—
HPP & Battery (D)	$K_e = 5.0$	−0.155+0.391i	0.368	0.062	16.083	0.319	1.000	0.824	0.217	0.018	0.015	Governor
		−4.968+2.256i	0.911	0.359	2.785	0.010	0.371	0.797	0.418	1.000	0.177	
		−0.352	1.000	0.000	2.841	0.848	1.000	0.606	0.143	0.010	0.014	
		−14.714	1.000	0.000	0.068	0.002	0.013	0.010	0.009	0.014	1.000	
HPP & Battery (PD)	$K_e = 2.5$, $M_e = 5.0$	−0.299+0.575i	0.462	0.091	10.932	0.085	1.000	0.974	0.409	0.053	0.023	Governor
		−5.003+2.290i	0.909	0.364	2.744	0.008	0.376	0.796	0.420	1.000	0.174	Water elasticity
		−0.161	1.000	0.000	6.2112	1.000	0.310	0.101	0.010	0.000	0.007	—
		−14.545	1.000	0.000	0.0688	0.009	0.013	0.010	0.009	0.014	1.000	—

One color represents an oscillation mode (OM), and the length of the color bar represents the relative size of the variable participation factor in each oscillation mode.

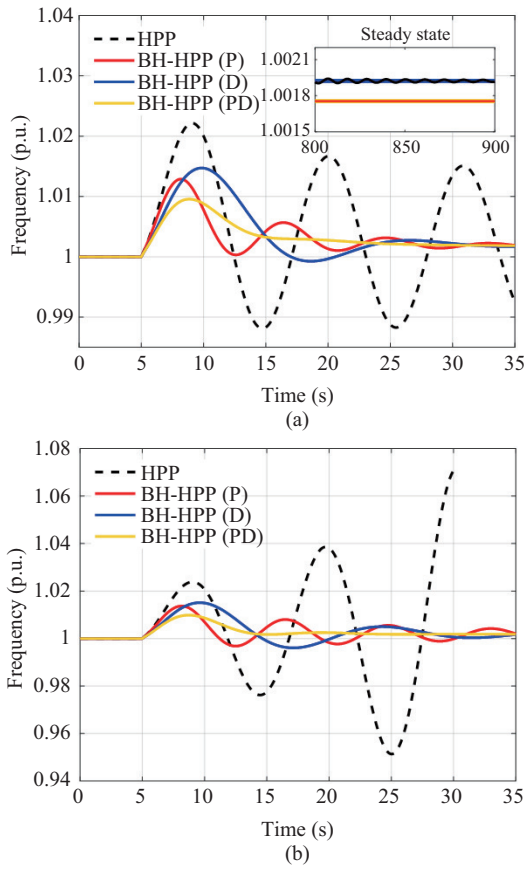

Fig. 11. Stability verification. (a) Frequency response in OP1. (b) Frequency response in OP2.

TABLE III
VALUES OF PFR PERFORMANCE EVALUATION INDEXES FOR OP1

Evaluation index	$\Delta f_{\max}$ (p.u.)	T_s (s)	$\Delta P_{\text{inv}-\max}$ (p.u.)	Δf_s (p.u.)
HPP	0.022	299.50	0.0364	0.0019
BH-HPP (P)	0.013	15.20	0.0075	0.0018
BH-HPP (D)	0.015	18.70	0.0000	0.0019
BH-HPP (PD)	0.010	11.70	0.0000	0.0018

In general, rapidity and stability contradict each other, but indexes of $\Delta f_{\max}$, T_s, and $\Delta P_{\text{inv}-\max}$ are all markedly improved by adding a battery to the system, indicating an evident improvement both in rapidity and stability for BH-HPP that cannot be achieved by conventional HPP. If virtual droop control is considered, Δf_s will be reduced and system steady-state performance is enhanced. For OP2, when assisted by a battery, HPP can rapidly become stable from its original unstable state with a similar dynamic performance described above. Numerical simulation results are in good agreement with theoretical analysis results in Section III.

To further reveal the PFR response mechanism of the BH-HPP, Fig. 12 shows the power output of systems under the three control strategies, in which the filled area is the penalty energy.

Due to water flow inertia (water hammer), there is an obvious reverse regulation, which is the main reason for the deterioration of regulation performance in HPPs. Since the battery can quickly respond to system requirements in the same direction at the initial stage of disturbance, it effectively counteracts reverse regulation of the BH-HPP (dotted line). When virtual inertia control is applied, the system's reverse regulation can even be completely offset. For virtual droop control, the battery eventually maintains an output, explaining why it can reduce steady-state error. For virtual inertia control, because the battery responds to frequency change rate while HPP mainly responds to frequency deviation, battery output is approximately in reverse phase with hydropower output. Although it leads to an increase in action amplitude and penalty energy of the HPP, fluctuation of the integrated system is mitigated. However, synthetic control combines the best of both and markedly improves transient processes of the hydropower system and implies less wear and tear on hydropower units.

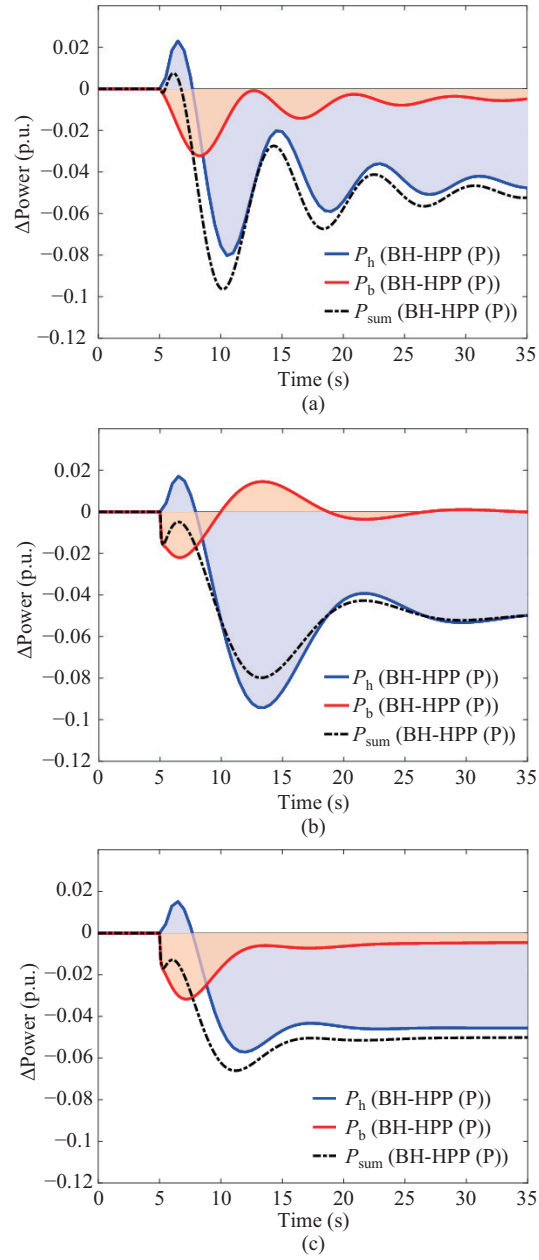

Fig. 12. Power simulation results. (a) Virtual droop control. (b) Virtual inertia control. (c) Synthetic control.

B. Discussion of Ancillary Battery Capacity

Indeed, the damping effect (K_e), inertial effect (M_e), and their percent contributions (a_m) to the BH-HPP are achieved by changing battery power, which is essentially the energy and sthe reserves capacity of the ancillary battery. Since both technical and economic factors have to be considered in the design capacity of battery devices, it is necessary to discuss how to limit the value of the control parameters. A small fluctuation of hydropower systems, i.e., the main PFR working condition, is generally defined as a load disturbance varying from 5% to 10%. If the HPP is in a critical steady state, with a 10% load disturbance as input, maximum charging or discharging battery power output in the PFR process can be obtained by simulation. Theoretically, the battery with a rated power exceeding this value can effectively assist the HPP in PFR. Besides, because the capacity of the battery with a certain discharge time depends on output power, the rated power represents battery capacity to a certain extent. Hence, in this paper, the maximum simulation power is considered as the designed rated power to reflect the capacity of the ancillary battery.

Figure 13(a) is the maximum simulation battery power when the BH-HPP is perturbed by a 10% load under different control parameters. Maximum battery power increases with K_e and M_e, indicating increase in battery capacity. If the rated power of the ancillary battery is assumed to be 5% of the HPP, the battery capacity-control parameter adaptive domain can be shown in Fig. 13(b). Only when K_e and M_e are adjusted in this domain, battery power will not be over-limited and the BH-HPP achieve good PFR performance. Similarly, battery capacity-control parameter adaptive domain under other battery capacity limitations can be obtained. In this paper, battery capacity can be simply obtained by a power output limitation.

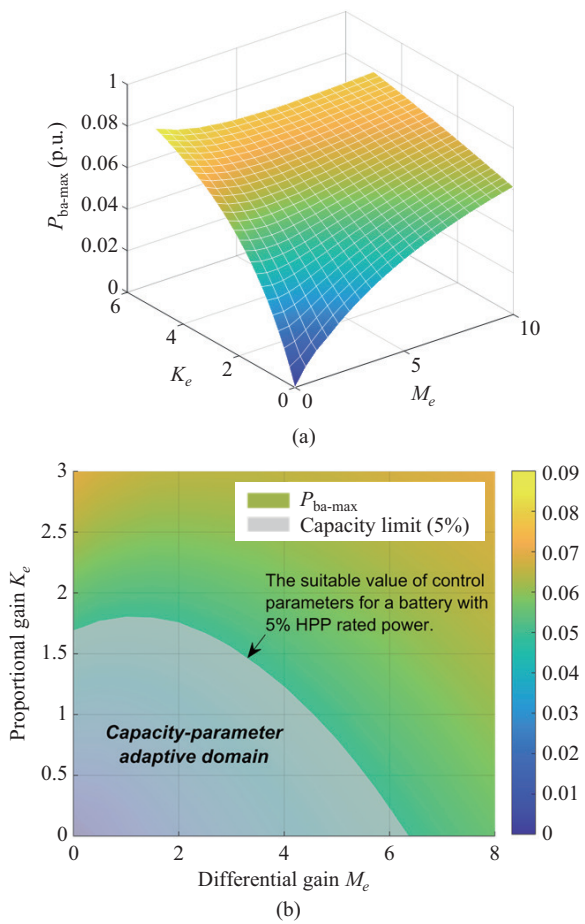

Fig. 13. Maximum simulation battery power in (a) PFR and (b) battery capacity-control parameter adaptive domain.

C. Case Study

In the last decade, the development of RESs has increased demand for better performance by frequency regulation power sources [35], [36]. Hence, a case study is carried out here to further investigate the advantages of the BH-HPP. The case is based on a hypothetical islanded hydro-wind hybrid system, as shown in Fig. 14(a), in which the HPP is the only regulator to smooth frequency fluctuation induced by the uncertainty of wind power.

The HPP model is based on prototype data of the real HPP mentioned in Section II, of which models of the turbine, pipeline, and generator systems are still linear with identical data in Table II except $e_y = 0.53$, $e_{\text{qy}} = 0.5325$, $e_h = 1.25$, $T_w = 1.0$ s and $T_a = 10.315$ s; while a refined governor model ($T_y = 0.368$ s) including dead band, saturation, rate limitation, and communication delay components is adopted to be the same as the real plant. Besides, the above-introduced battery model with a 5% hydropower capacity is applied in the BH-HPP scenario. As for the wind farm, it is simplified to a disturbance source by using actual normalized wind power data (from a grid in China, as shown in Fig. 14(b)).

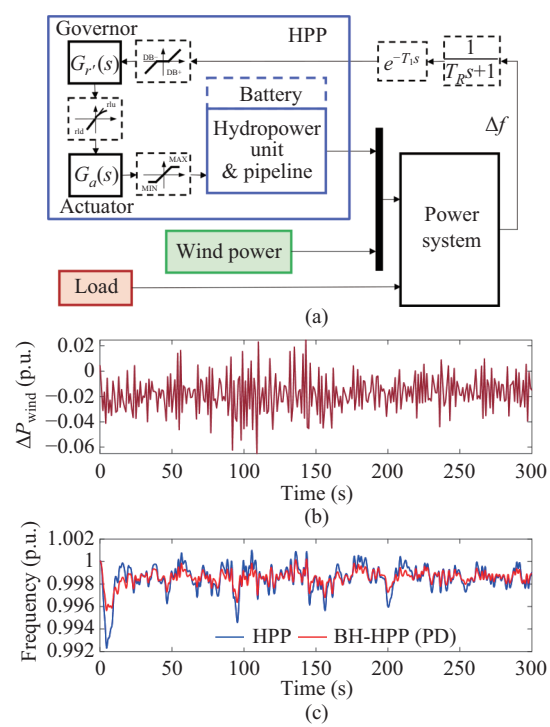

Fig. 14. Case: (a) an islanded hydro-wind hybrid system, (b) the wind power deviation and (c) frequency response of the case power system.

The simulation result for the BH-HPP (synthetic control) is shown in Fig. 14(c). Even though the turbine governor is set to be in a well-stable state ($K_p = 6.0$, $K_i = 1.5$), frequency response is still notably improved especially in relatively large disturbances after being assisted by the battery (red line).

VI. Discussion

Compared with current HPPs equipped with conventional hydropower units, the performance improvements of the BH-HPP in the PFR process proposed in this paper are discussed as follows:

1) Stability: The stability region of isolated BH-HPP for PFR is theoretically derived and intuitively plotted. Through analysis of the frequency-domain and root locus, it is proved the ancillary battery at the unit side can notably expand the stability of HPPs.

2) Rapidity: Time-domain simulation results and participation factor analysis argue that the negligible ramp rate of the unit-side battery effectively improves the frequency response speed of the hydropower unit. It offers the hydropower system near-instant response speed for PFR while retaining large capacity advantages.

3) Transient: From the aspect of overall output, the hybrid unit can even counterbalance the inherent reverse regulation of hydropower units due to flow inertia; from the perspective of hydropower units, the ancillary battery shares regulation burden, which provides a feasible tack for further study of utilizing battery to reduce unit wear and tear.

Meanwhile, there are several limitations in this work, and some aspects can be further researched in the future.

1) The linearized small disturbance model is used for theoretical analysis in this paper. However, in practical operation, some nonlinear factors may affect the regulation effect, such as turbine characteristic curves and battery efficiency.

2) Capacity planning and detailed control of the ancillary battery is less discussed. In the future, battery performance management should be further considered.

3) For now, research is a prospective theoretical study of battery ancillary frequency regulation in hydropower systems. To enhance reliability, physical model experiments are our ongoing and future work.

VII. Conclusion

By hybridizing a battery on the unit side to assist hydropower, the PFR performance of HPPs can be vastly improved. Contents of this paper mainly include the following aspects:

1) Model integration: A battery hybridized hydropower plant model with linear characteristics but sufficient accuracy is established in this paper, in which the HPP model is validated by field-measured data and the simplified battery model is verified based on a standard detailed model.

2) Theoretical understanding: The mechanism of this new hydropower flexibility enhancement solution is studied by theoretical analysis and numerical simulation. Even a small-sized battery can help conventional HPPs overcome the contradiction between rapidity and stability in PFR, because the battery's negligible ramp rates not only notably improve response speed but also markedly broaden the stability region of turbine governor parameters.

3) Research inspiration: Systems under different common battery control strategies show unique characteristics, and synthetic control strategy demonstrates the best results; besides, battery capacity should be considered in the tuning of control parameters. BH-HPP also shows good performance in a RES scenario case. Refined controls combined with battery operation and hydropower characteristics should be included in future work.

References

[1] Q. Guo, F. Xiao, C. M. Tu, F. Jiang, R. W. Zhu, J. Ye, and J. Y. Gao, "An overview of series-connected power electronic converter with function extension strategies in the context of high-penetration of power electronics and renewables," *Renewable and Sustainable Energy Reviews*, vol. 156, pp. 111934, Mar. 2022.

[2] W. J. Yang, P. Norrlund, L. Saarinen, A. Witt, B. Smith, J. D. Yang, and U. Lundin, "Burden on hydropower units for short-term balancing of renewable power systems," *Nature Communications*, vol. 9, no. 1, pp. 2633, Jul. 2018.

[3] J. P. Hoffstaedt, D. P. K. Truijen, J. Fahlbeck, L. H. A. Gans, M. Qudaih, A. J. Laguna, J. D. M. De Kooning, K. Stockman, H. Nilsson, P. T. Storli, B. Engel, M. Marence, and J. D. Bricker, "Low-head pumped hydro storage: a review of applicable technologies for design, grid integration, control and modelling," *Renewable and Sustainable Energy Reviews*, vol. 158, pp. 112119, Apr. 2022.

[4] D. Valentín, A. Presas, M. Egusquiza, J. L. Drommi, and C. Valero, "Benefits of battery hybridization in hydraulic turbines. Wear and tear evaluation in a Kaplan prototype," *Renewable Energy*, vol. 199, pp. 35–43, Nov. 2022.

[5] HydroWIRES Initiative Research Roadmap. (2022). U.S. Department of Energy, America. [Online]. Available: https://www.energy.gov/sites/default/files/2022-02/HydroWIRES%20Roadmap%20FINAL%20%28508%20Compliant%29_0.pdf.

[6] WORLD-ENERGY. (2021, Aug.). RWE combines hydropower with mega-batteries to balance grid. [Online]. Available: https://www.world-energy.org/article/19733.html.

[7] X. D. Lu, C. S. Li, D. Liu, Z. W. Zhu, and X. Q. Tan, "Influence of water diversion system topologies and operation scenarios on the damping characteristics of hydropower units under ultra-low frequency oscillations," *Energy*, vol. 239, pp. 122679, Jan. 2022.

[8] W. J. Yang, P. Norrlund, J. Bladh, J. D. Yang, and U. Lundin, "Hydraulic damping mechanism of low frequency oscillations in power systems: quantitative analysis using a nonlinear model of hydropower plants," *Applied Energy*, vol. 212, pp. 1138–1152, Feb. 2018.

[9] J. J. Zhang, A. Mahmud, W. Govaerts, D. Y. Chen, B. B. Xu, and H. L. Xiong, "Sensitivity analysis and low frequency oscillations for bifurcation scenarios in a hydraulic generating system," *Renewable Energy*, vol. 162, pp. 334–344, Dec. 2020.

[10] L. Saarinen, P. Norrlund, W. J. Yang, and U. Lundin, "Allocation of frequency control reserves and its impact on wear and tear on a hydropower fleet," *IEEE Transactions on Power Systems*, vol. 33, no. 1, pp. 430–439, Jan. 2018.

[11] L. M. Chen, X. Lu, Y. Min, Y. W. Zhang, Q. Chen, Y. M. Zhao, and C. Ben, "Optimization of governor parameters to prevent frequency oscillations in power systems," *IEEE Transactions on Power Systems*, vol. 33, no. 4, pp. 4466–4474, Jul. 2018.

[12] Z. G. Zhao, J. D. Yang, Y. F. Huang, W. J. Yang, W. C. Ma, L. Y. Hou, and M. Chen, "Improvement of regulation quality for hydro-dominated power system: quantifying oscillation characteristic and multi-objective optimization," *Renewable Energy*, vol. 168, pp. 606–631, May 2021.

[13] G. Chen, F. Tang, H. B. Shi, R. Yu, G. H. Wang, L. J. Ding, B. S. Liu, and X. N. Lu, "Optimization strategy of hydrogovernors for eliminating ultralow-frequency oscillations in hydrodominant power systems," *IEEE Journal of Emerging and Selected Topics in Power Electronics*, vol. 6, no. 3, pp. 1086–1094, Sep. 2018.

[14] N. Kishor, R. P. Saini, and S. P. Singh, "A review on hydropower plant models and control," *Renewable and Sustainable Energy Reviews*, vol. 11, no. 5, pp. 776–796, Jun. 2007.

[15] W. J. Yang, Y. F. Huang, Z. G. Zhao, J. D. Yang, and J. B. Yang, "Stability region of hydropower plant with surge tank at HVDC sending terminal," *Energy Science & Engineering*, vol. 9, no. 5, pp. 694–709, May 2021.

[16] W. C. Wu, X. R. Wang, and X. Xiao, "Multiple DC coordinated suppression method for ultra-low frequency oscillations," *Sustainable Energy Technologies and Assessments*, vol. 53, pp. 102301, Oct. 2022.

[17] J. I. Pérez-Díaz, M. Lafoz, and F. Burke, "Integration of fast acting energy storage systems in existing pumped-storage power plants to enhance the system's frequency control," *WIREs Energy and Environment*, vol. 9, no. 2, pp. e367, Mar./Apr.. 2020.

[18] C. L. Jin, N. Lu, S. Lu, Y. Makarov, and R. A. Dougal, "Coordinated control algorithm for hybrid energy storage systems," in *2011 IEEE Power and Energy Society General Meeting*, 2011, pp. 1–7.

[19] C. L. Jin, N. Lu, S. Lu, Y. V. Makarov, and R. A. Dougal, "A coordinating algorithm for dispatching regulation services between slow and fast power regulating resources," *IEEE Transactions on Smart Grid*, vol. 5, no. 2, pp. 1043–1050, Mar. 2014.

[20] V. Gevorgian, E. Muljadi, Y. S. Luo, M. Mohanpurkar, R. Hovsapian, and V. Koritarov, "Supercapacitor to provide ancillary services," in *2017 IEEE Energy Conversion Congress and Exposition (ECCE)*, 2017, pp. 1030–1036.

[21] J. Kim, V. Gevorgian, Y. S. Luo, M. Mohanpurkar, V. Koritarov, R. Hovsapian, and E. Muljadi, "Supercapacitor to provide ancillary services with control coordination," *IEEE Transactions on Industry Applications*, vol. 55, no. 5, pp. 5119–5127, Sep./Oct. 2019.

[22] T. Mäkinen, A. Leinonen, and M. Ovaskainen, "Modelling and benefits of combined operation of hydropower unit and battery energy storage system on grid primary frequency control," in *2020 IEEE International Conference on Environment and Electrical Engineering and 2020 IEEE Industrial and Commercial Power Systems Europe (EEEIC / I&CPS Europe)*, 2020, pp. 1–6.

[23] S. Cassano and F. Sossan, "Model predictive control for a medium-head hydropower plant hybridized with battery energy storage to reduce penstock fatigue," *Electric Power Systems Research*, vol. 213, pp. 108545, Dec. 2022.

[24] A. Schreider and R. Bucher, "An auspicious combination: fast-ramping battery energy storage and high-capacity pumped hydro," *Energy Procedia*, vol. 155, pp. 156–164, Nov. 2018.

[25] T. Ma, H. X. Yang, and L. Lu, "Feasibility study and economic analysis of pumped hydro storage and battery storage for a renewable energy powered island," *Energy Conversion and Management*, vol. 79, pp. 387–397, Mar. 2014.

[26] M. S. Javed, D. Zhong, T. Ma, A. T. Song, and S. Ahmed, "Hybrid pumped hydro and battery storage for renewable energy based power supply system," *Applied Energy*, vol. 257, pp. 114026, Jan. 2020.

[27] M. Guezgouz, J. Jurasz, B. Bekkouche, T. Ma, M. S. Javed, and A. Kies, "Optimal hybrid pumped hydro-battery storage scheme for off-grid renewable energy systems," *Energy Conversion and Management*, vol. 199, pp. 112046, Nov. 2019.

[28] W. J. Yang, J. D. Yang, W. Zeng, R. B. Tang, L. Y. Hou, A. T. Ma, Z. G. Zhao, and Y. M. Peng, "Experimental investigation of theoretical stability regions for ultra-low frequency oscillations of hydropower generating systems," *Energy*, vol. 186, pp. 115816, Nov. 2019.

[29] W. J. Yang, P. Norrlund, L. Saarinen, J. D. Yang, W. Zeng, and U. Lundin, "Wear reduction for hydropower turbines considering frequency quality of power systems: a study on controller filters," *IEEE Transactions on Power Systems*, vol. 32, no. 2, pp. 1191–1201, Mar. 2017.

[30] A. Oshnoei, M. Kheradmandi, F. Blaabjerg, N. D. Hatziargyriou, S. M. Muyeen, and A. Anvari-Moghaddam, "Coordinated control scheme for provision of frequency regulation service by virtual power plants," *Applied Energy*, vol. 325, pp. 119734, Nov. 2022.

[31] Z. G. Zhao, J. D. Yang, C. Y. Chung, W. J. Yang, X. H. He, and M. Chen, "Performance enhancement of pumped storage units for system frequency support based on a novel small signal model," *Energy*, vol. 234, pp. 121207, Nov. 2021.

[32] F. Golnaraghi and B. C. Kuo, *Automatic Control Systems*, 10th ed., Hoboken: McGraw-Hall, 2017.

[33] W. J. Yang, J. D. Yang, W. C. Guo, and P. Norrlund, "Frequency stability of isolated hydropower plant with surge tank under different turbine control modes," *Electric Power Components and Systems*, vol. 43, no. 15, pp. 1707–1716, Aug. 2015.

[34] P. Kundur, *Power System Stability and Control*, New York: McGraw-Hill, 1994.

[35] S. Zhang, Y. Xiang, J. Y. Liu, J. C. Liu, J. X. Yang, X. Zhao, S. Jawad, and J. Wang, "A regulating capacity determination method for pumped storage hydropower to restrain PV generation fluctuations," *CSEE Journal of Power and Energy Systems,* vol. 8, no. 1, pp. 304–316, Jan. 2022.

[36] C. Wu, X. P. Zhang, and M. Sterling, "Wind power generation variations and aggregations," *CSEE Journal of Power and Energy Systems,* vol. 8, no. 1, pp. 17–38, Jan. 2022.

Yiwen Liao received the B.S. degree in Water conservancy and Hydropower Engineering from Wuhan University in 2021. Currently, he is pursuing the M.S degree in the State Key Laboratory of Water Resources and Hydropower Engineering Science, Wuhan University, Hubei, China. His research interests include the dynamics and control of hydropower systems, and the modeling and regulation of hydro/wind/PV/storage hybrid systems.

Weijia Yang received his B.S. and M.S. degrees from School of Water Resources and Hydropower Engineering, Wuhan University, Wuhan, China in 2011 and 2013, respectively. He obtained his Ph.D. degree in 2017 at Division of Electricity, Department of Engineering Sciences, Uppsala University, Uppsala, Sweden. He is presently working as an Associate Professor at the State Key Laboratory of Water Resources and Hydropower Engineering Science in Wuhan University, Wuhan, China. He is a member of IEC/TC4/WG 36 and the IAHR, etc. He mainly works on the dynamics and control of hydropower system, in the interdisciplinary field regarding hydraulics, mechanics and electrical engineering. His current research interests include large-scale hydropower plants, hydro/wind/PV/storage hybrid systems, and variable speed pumped storage, etc.

Zhecheng Wang received the B.S. degree in Water conservancy and Hydropower Engineering from Wuhan University in 2022. Currently, he is pursuing the M.S degree in the State Key Laboratory of Water Resources and Hydropower Engineering Science, Wuhan University, Hubei, China. His research interest is the regulation of hydropower and battery combined hybrid systems.

Yifan Huang received the B.S. from the School of Water Resources and Hydropower Engineering, Wuhan University, Wuhan, China, in 2020. He is currently working toward the M.S. degree in the State Key Laboratory of Water Resources and Hydropower Engineering Science, Wuhan University, Hubei, China. He is a young professional member of the International Association for Hydro-Environment Engineering and Research. His research interests include transient process and control of hydropower plants and variable speed pumped storage plants.

C. Y. Chung received the B.Eng. (with First Class Honors) and Ph.D. degrees in Electrical Engineering from The Hong Kong Polytechnic University, Hong Kong, China, in 1995 and 1999, respectively. He is currently the Head of Department and Chair Professor of Power Systems Engineering in the Department of Electrical Engineering at the Hong Kong Polytechnic University, Hong Kong, China. His research interests include smart grid technologies, renewable energy, power system stability/control, planning and operation, computational intelligence applications, power markets and electric vehicle charging. Dr. Chung is a Senior Editor of "IEEE Transactions on Power Systems", Consulting Editor of "IEEE Transactions on Sustainable Energy", and Vice Editor-in-Chief of "Journal of Modern Power Systems and Clean Energy". He is an IEEE PES Distinguished Lecturer. He is also the recipient of the 2021 IEEE Canada P. Ziogas Electric Power Award.